Electronic Supplemental Information

Directed flexibility: Self-assembly of a supramolecular tetrahedron

James M. Ludlow III,[a] Tingzheng Xie,[a] Zaihong Guo, Kai Guo,[a] Mary J. Saunders[c], Charles N. Moorefield,[c] Chrys Wesdemiotis,*[a,b] and George R. Newkome*[a,b]

[a]*Department of Polymer Science,* [b]*Department of Chemistry, and* [c]*The Maurice Morton Institute for Polymer Science The University of Akron, Akron, OH 44325-4717 USA*
Tel: 330-972-6458
E-mail: newkome@uakron.edu, wesdemiotis@uakron.edu

Table of Contents

1. General Procedures

Chemicals were commercially purchased and used without further purification. Thin layer chromatography (TLC) was conducted on flexible sheets (Baker-flex) precoated with Al_2O_3 (IB-F) or SiO_2 (IB2-F) and visualized by UV light. Column chromatography was conducted using basic Al_2O_3, Brockman Activity I (60-325 mesh) or SiO_2 (60-200 mesh) from Fisher Scientific. ^1H NMR spectra were recorded on a Varian 500 MHz spectrometer. Variable temperature NMR experiments were conducted on a Varian 400 MHz NMR spectrometer; the temperature was varied in 10 °C increments. Electrospray ionization (ESI) mass spectra (MS) were obtained on a Synapt HDMS quadrupole/time-of-flight (Q/ToF) mass spectrometer (Waters Corp., Milford, MA). The Synapt Q/ToF instrument contains a travelling wave ion mobility (TWIM) device in the interface region between the Q and ToF mass analyzers, consisting of three confined regions arranged in the order trap cell (closest to Q), ion mobility (IM) cell, and transfer cell (closest to ToF). Trap and transfer cells can be used as collision cells for tandem mass spectrometry (MS^2) experiments before or after IM separation, respectively. In the IM cell, the ions drift under influence of a traveling wave (*i.e.* pulsed) field against the flow of a carrier gas (N_2). This process disperses ions based on their mass, charge, and shape. The separated ions travel through the transfer cell from which they are conveyed to the orthogonal ToF analyzer for *m/z* measurement. The acquired data are typically displayed in 2-D plots of *m/z* ratio *vs.* the corresponding drift time through the IM cell. The TWIM-MS experiments were performed under the following conditions: ESI capillary voltage, 1 kV; sample cone voltage, 8 V; extraction cone voltage, 3.2 V; desolvation gas flow, 800 L/h (N_2); trap collision energy (CE), 3 eV; transfer CE, 1 eV; trap gas flow, 1.5 mL/min (Ar); TWIM cell gas flow, 22.7 mL/min (N_2); sample flow rate, 5 μL/min; source temperature,

30 °C; desolvation temperature, 40 °C; TWIM wave height, 7.5 V; and TWIM wave velocity, 350 m/s. In the gradient tandem mass spectrometry (gMS^2) experiments, a specific charge state, selected by the Q mass analyzer, was fragmented by CAD with Ar atoms in the trap cell and the resulting fragments plus any undissociated precursor ions were separated by their ion mobilities in the IM cell before ToF mass analysis. The laboratory-frame collision energy (E_{lab}) was varied by adjusting the potential of the trap cell (V_{trap}) between 15 and 80 V. The E_{lab} energy gained in this process is equal to *z* (ion charge) x V_{trap}; the corresponding center-of-mass energy (E_{cm}) can be calculated *via* $E_{cm} = E_{lab} \times m/(m+M)$, where m is the mass of the collision gas atoms (40 Da) and M is the mass of the ions. ESI-MS, TWIM-MS, and gMS^2 data analyses were conducted using the MassLynx 4.1 and DriftScope 2.1 programs provided by Waters.

Molecular Modeling. Energy minimization of structures was conducted with the Materials Studio version 6.0 program using the Anneal and Geometry Optimization tasks in the Forcite module (Accelrys Software, Inc.). The counterions were omitted. An initially energy-minimized structure was subjected to 10 annealing cycles with initial and mid-cycle temperatures of 300 and 500 K, respectively, five heating ramps per cycle, one hundred dynamics steps per ramp, and one dynamics step per femtosecond. Constant volume/constant energy (NVE) ensemble was used; the geometry was optimized after each cycle. All geometry optimizations used a universal force field with atom-based summation and cubic spline truncation for both the electrostatic and van der Waals parameters. 50 candidate structures were generated for the calculation of collision cross sections.

Collision Cross-section (CCS) Calibration. The drift time scale of the TWIM-MS experiments was converted to a collision cross-section scale by calibration with ions of known CCS, following the procedure established by Ruotolo et al.[3] Briefly, the corrected collision cross sections of the molecular ions of insulin (bovine pancreas), ubiquitin (bovine red blood cells), and cytochrome C (horse heart), obtained from published work,[2] were plotted against the corrected drift times (arrival times) of the corresponding molecular ions measured in TWIM-MS experiments at the same traveling-wave velocity, traveling-wave height and ion-mobility gas flow settings, *viz.* 350 ms^{-1}, 7.5 V and 22.7 mL min^{-1}. All charge states observed for the calibrants were used in the construction of the curve.

2. Synthetic Procedures

Tribenzo-27-crown-9 (**3**) was synthesized and characterized according to the literature.[1]

2,3,13,14,24,25–Hexabromo-6,7,9,10,17,18,20,21,28,29,31,32-dodecahydrotribenzo[*b*,*k*,*t*][1,4,7,10,13,16,19,22,25]nonaoxacycloheptacosine (**4**)**:** To a stirred solution of **1** (480 mg, 880 μmol) and I_2 (9 mg, 36 μmol) in CH_2Cl_2 (50 mL), a solution of Br_2 (1.06 g, 6.66 mmol) in CH_2Cl_2 (15 mL) was added dropwise over one hour. This solution was maintained at 25 °C for an additional 7 h. The mixture was dried *in vacuo* to give a solid, which was recrystallized from EtOH to give (82%) of **4**, as a colorless solid: 740 mg, m.p. 152-153°C; ^{1}H NMR ($CDCl_3$, 500 MHz, ppm): 7.11 (s, 6H), 4.10 (m, 12H,

ArOCH_2), 3.90 (m, 12H, ArOCH$_2$CH_2); ^{13}C NMR (125 MHz, $CDCl_3$, ppm): 148.76, 118.98, 115.45, 69.92, 69.61; MALDI-MS (*m/z*): 1036.9 [M+Na] (Calcd. = 1036.7).

2,3,13,14,24,25–Hexa*kis*(4-[2,2':6',2'']terpyridin-4'-ylphenyl)-6,7,9,10,17,18,20,-21,28,29,31,32-dodecahydrotribenzo[*b*,*k*,*t*][1,4,7,10,13,16,19,22,25]nonaoxacyclo-heptacosine (**5**): A mixture of **4** (322 mg, 318 μmol), (4-[2,2':6',2"]-terpyridin-4'-ylphenyl)boronic acid (1.009 g, 2.86 mmol), $Pd(PPh_3)_2Cl_2$ (135 mg, 190 μmol), and Na_2CO_3 (504 mg, 4.74 μmol) was added to a dry round bottom flask, which was then evacuated and backfilled with Argon (5X). A mixture of toluene (150 mL), MeOH (60 mL), and H_2O (90 mL) was degassed with Argon for 15 min then added to the flask, under Argon. The resultant mixture was refluxed for 60 h, then cooled. The aqueous layer was extracted with $CHCl_3$ and then combined with the organic layer. The solution was dried ($MgSO_4$), filtered, and concentrated to dryness. The resultant solid was column chromatographed (Al_2O_3) using $CHCl_3$/EtOAc/hexanes (1:1:1), followed by pure $CHCl_3$ to give (43%) **5**, as a colorless solid: 325 mg, m.p. 218-220 °C; ^{1}H NMR ($CDCl_3$, 500 MHz, ppm): 8.70 (s, 12H, 3',5'-tpy*H*), 8.65 (d, J = 5 Hz, 6,6"-tpy*H*, 12H), 8.60 (d, J = 8 Hz, 3,3"-tpy*H*, 12H), 7.77 (dd, $J_1 = J_2$ = 8 Hz, 4,4"-tpy*H*, 12H), 7.73 (d, J = 8 Hz, 12H), 7.23 - 7.31 (m, 32H), 7.14 (s, 6H), 4.34 (t, J = 5 Hz, 12H), 4.09 (t, J = 5 Hz, 12H); ^{13}C NMR (125 MHz, $CDCl_3$, ppm): 69.65, 70.29, 117.24, 118.75, 121.24, 123.62, 126.95, 130.41, 133.28, 136.24, 136.69, 142.00, 148.62, 149.05, 149.72, 155.78, 156.29; MALDI-MS (*m/z*): 2382.9 (Calcd. *m/z* = 2382.9)

Self-assembly to tetrahedral structure L4M12: To a stirred solution of **5** (21.3 mg, 8.91 μmol) in $CHCl_3$/MeOH (3:2, 20 mL) at 25 °C, a 250 mM solution of $Zn(NO_3)_2 \cdot 6H_2O$ in MeOH (1.062 mL) was added. After 30 min, NH_4PF_6 (90 mg) was

added. The resultant yellow precipitate was filtered, washed with MeOH and H_2O, then dried *in vacuo* to give (84%) **L4M12**, as a yellow solid: 25.9 mg, m.p. >300°C; ^{1}H NMR (CD_3CN/DMF-d_7, 500 MHz, ppm): 8.97 (s, 48H, 3',5'-tpy*H*), 8.64 (d, *J* = 8 Hz, 48H, 3, 3"-tpy*H*), 8.13 (d, *J* = 8 Hz, 4H, Ar*H*), 7.64 - 7.77 (m, 96H, 6,6"-tpy*H*, 4,4"-tpy*H*), 7.58 (d, *J* = 8 Hz, 48H, Ar*H*), 7.33 (s, 24H, Ar*H*), 6.86 (m, 48H, 5,5"-tpyH), 4.59 - 4.71 (m), 4.34 - 4.44 (m), 4.13 - 4.24 ppm (m), 4.04 - 4.13 ppm (m);^{1}H NMR (CD_3CN/DMSO-d_6, 500 MHz, ppm): 8.92 (s, 48H, 3',5'-tpy*H*), 8.56 (d, *J* = 8 Hz, 48H, 3, 3"-tpy*H*), 8.08 (d, *J* = 8 Hz, 4H, Ar*H*), 7.56 - 7.67 (m, 96H, 4,4"-tpy*H*, 6,6" -tpy*H*), 7.53 (d, *J* = 8 Hz, 48H, Ar*H*), 7.28 (s, 24H, Ar*H*), 6.73 - 6.83 (m, 48H, 5,5" -tpy*H*), 4.50 - 4.66 (m), 4.24 - 4.38 (m), 3.96 - 4.17 ppm (m); ESI-MS (*m/z*) 1235.1 $[M\text{-}10PF_6]^{10+}$ (Calcd. *m/z* = 1235.2), 1388.4 $[M\text{-}9PF_6]^{9+}$ (Calcd. *m/z* = 1388.6), 1580.1 $[M\text{-}8PF_6]^{8+}$ (Calcd. *m/z* = 1580.4), 1826.7 $[M\text{-}7PF_6]^{7+}$ (Calcd. *m/z* = 1826.9), 2155.1 $[M\text{-}6PF_6]^{6+}$ (Calcd. *m/z* = 2155.4), 2615.8 $[M\text{-}5PF_6]^{5+}$ (Calcd. *m/z* = 2615.6).

To obtain L4M12 possessing tetra*kis*(perfluorophenyl)borate counterions, potassium tetra*kis*(perfluorophenyl)borate was used in place of NH_4PF_6 gave (82%); ^{1}H NMR (CD_3CN/DMF-d_7, 500 MHz, ppm): 9.08 (s, 48H, 3',5'-tpy*H*), 8.74 (d, *J* = 8 Hz, 48H, 3,3"-tpy*H*), 8.17 (d, *J* = 8 Hz, 48H, Ar*H*), 7.73 (d, *J* = 5 Hz, 48H, 6,6"-tpy*H*), 7.61 (dd, $J_1 = J_2$ = 8 Hz, 48H, 4,4"-tpy*H*), 7.52 (d, *J* = 8 Hz, 48H, Ar*H*), 7.29 (s, 24H, Ar*H*), 6.82 (m, 48H, 5,5"-tpyH), 4.66 - 4.55 (m), 4.40 - 4.32 (m), 4.18 - 4.10 ppm (m), 4.10 - 4.00 ppm (m).

Self-assembly of model complex 2 was synthesized and characterized according to the literature.[2] To obtain complex **2** with tetra*kis*(perfluorophenyl)borate counterion, potassium tetra*kis*(perfluorophenyl)borate (BARF) was used in place of NH_4PF_6. ^{1}H NMR (CD_3CN/DMF-d_7, 500 MHz, ppm): 9.08 (s, 12H, 3',5'-tpy*H*), 8.80 (d, *J* = 8 Hz,

12H, 3,3"-tpy*H*), 8.16 (d, J = 8 Hz, 12H, Ar*H*), 8.06 (dd, J_1=J_2 = 8 Hz, 12H, 4,4"-tpy*H*), 7.85 (d, J = 5 Hz, 12H, 6,6"-tpy*H*), 7.61 (d, J = 8, 12H, Ar*H*), 7.32 (dd, J_1 = 8 Hz, J_2 = 5 Hz, 12H, 5,5"-tpyH), 7.21 (s, 6H, Ar*H*), 4.00 (s, 9H, OCH_3); ESI-MS (*m/z*) 409.1 [M - 6BARF]$^{6+}$ (Calcd. *m/z* = 408.7); 626.7 [M - 5BARF]$^{5+}$ (Calcd. *m/z* = 626.2); 953.0 [M - 4BARF]$^{4+}$ (Calcd. *m/z* = 952.5); 1497.0 [M - 3BARF]$^{3+}$ (Calcd. *m/z* = 1496.3)

3. NMR Spectra

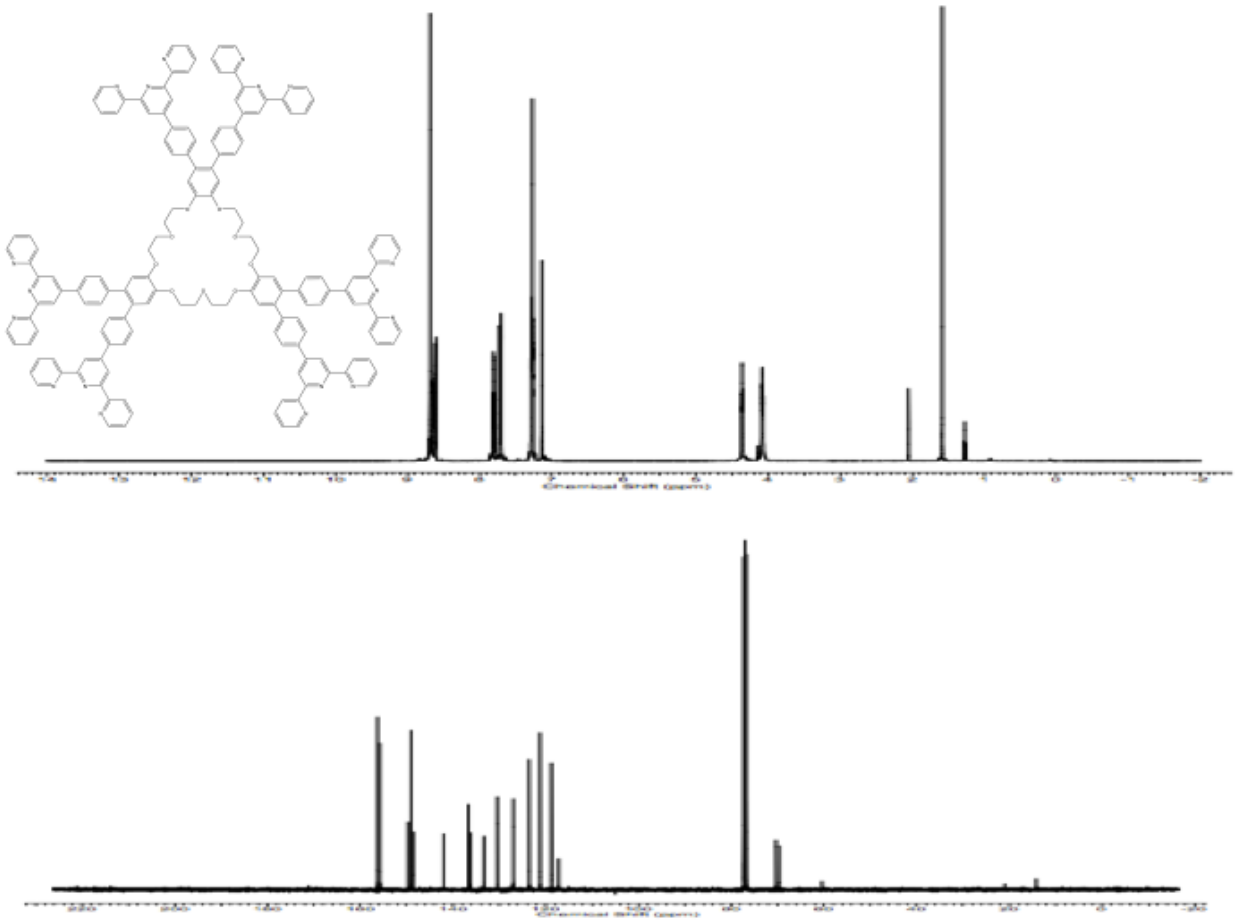

Figure S1. Proton and carbon (**5**) NMR in $CDCl_3$ at 20 °C and 10 mg/mL

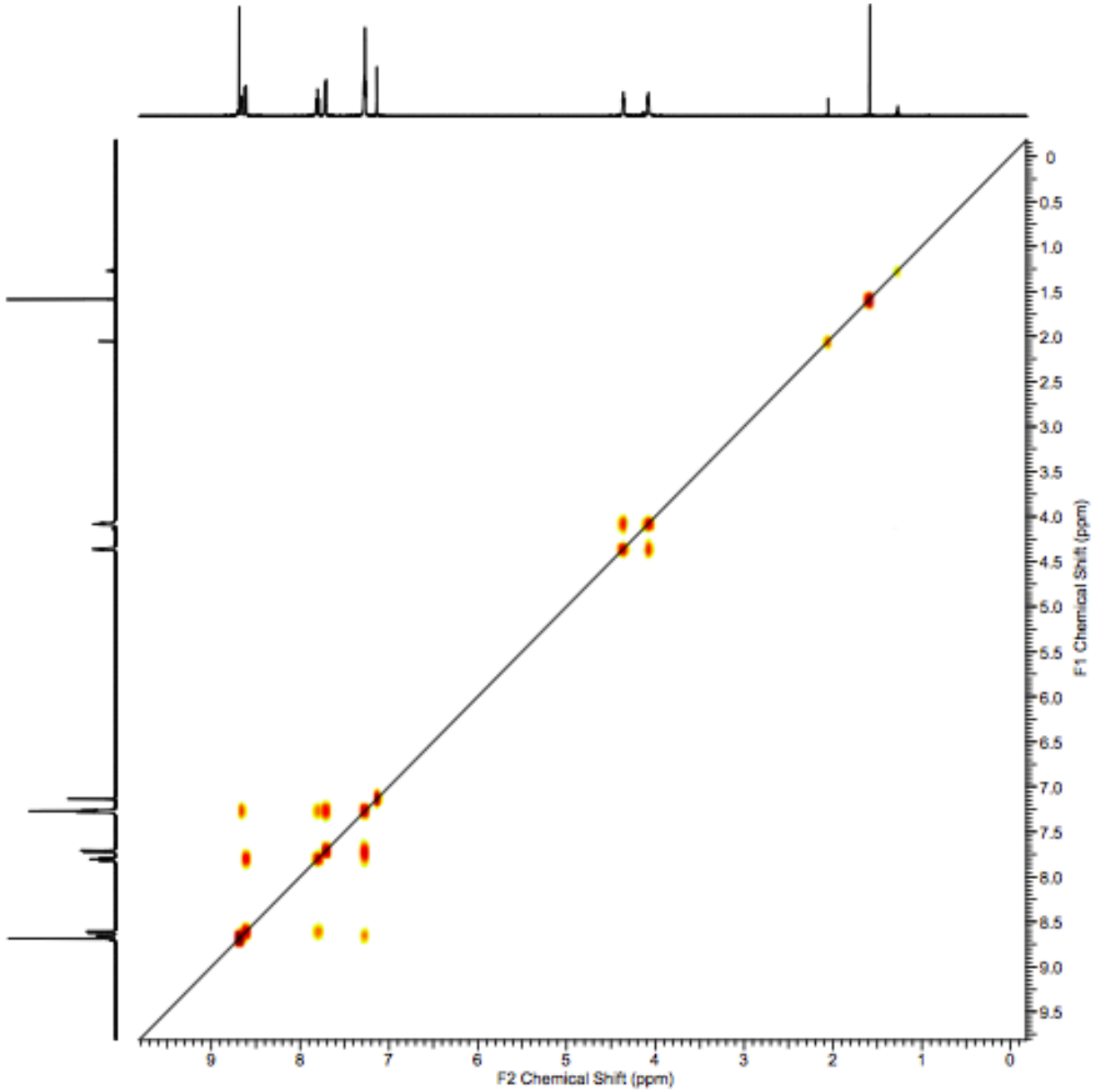

Figure S2. COSY for **5** in $CDCl_3$ at 20 °C and 10 mg/mL

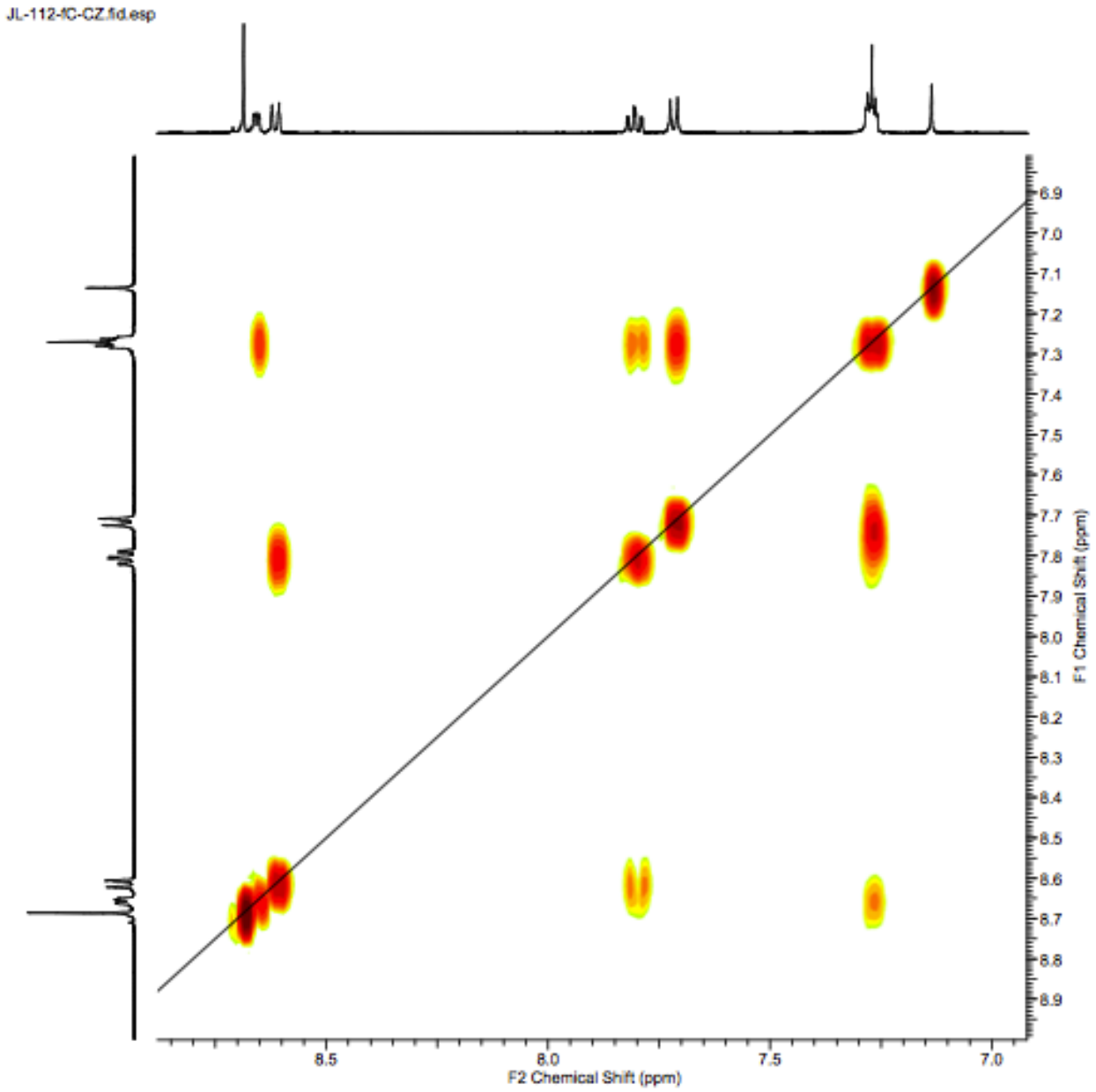

Figure S3. COSY for **5** aromatic region in $CDCl_3$ at 20 °C and 10 mg/mL

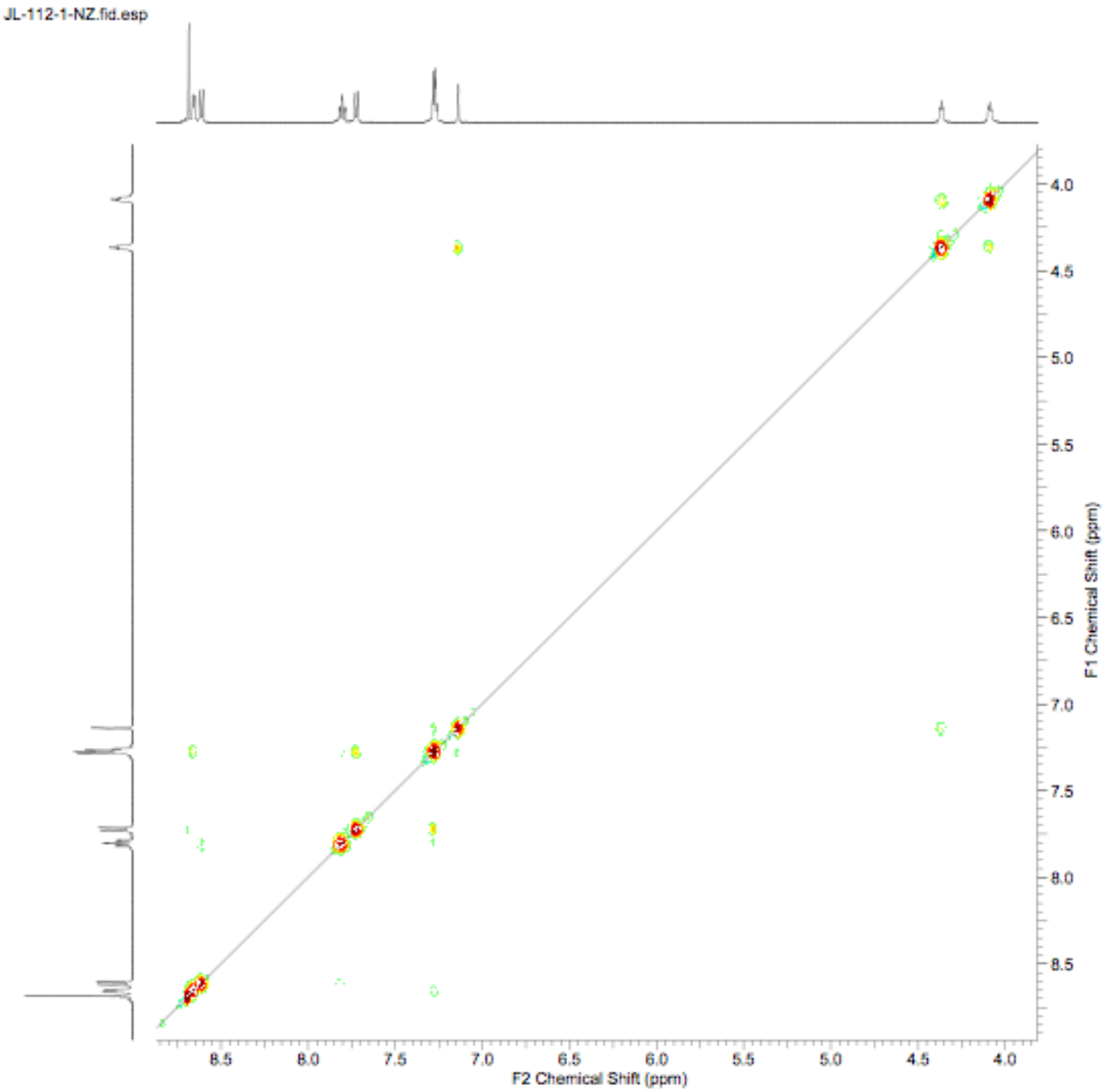

Figure S4. NOESY for **5** in $CDCl_3$ at 20 °C and 10 mg/mL

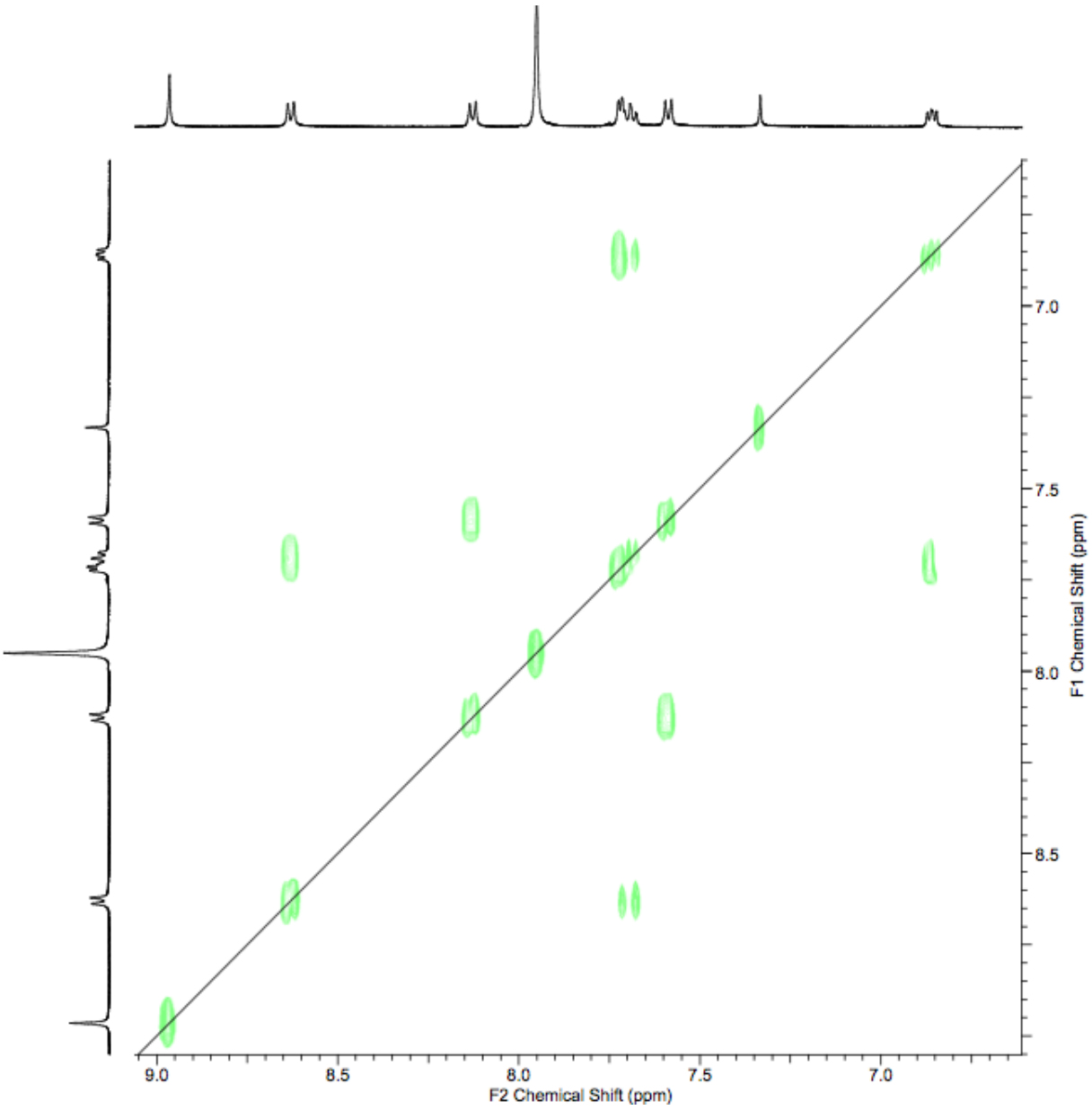

Figure S5. COSY for **L4M12**, aromatic region CD_3CN/DMF-d_7.(5:1) at 0.6 mg/mL and 20 °C

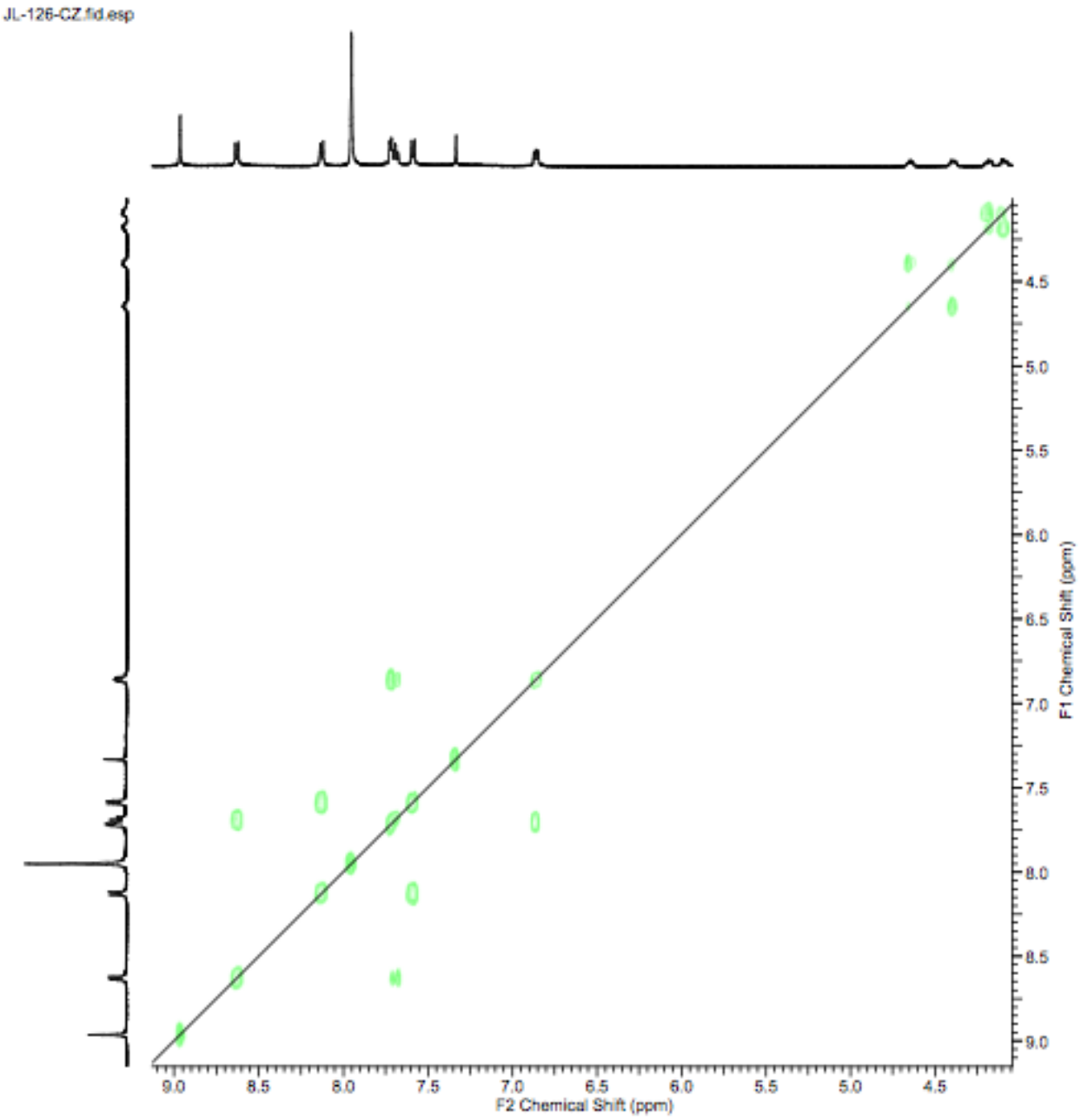

Figure S6. COSY for **L4M12**, aromatic and marker region CD_3CN/DMF-d_7.(5:1) at 0.6 mg/mL and 20 °C

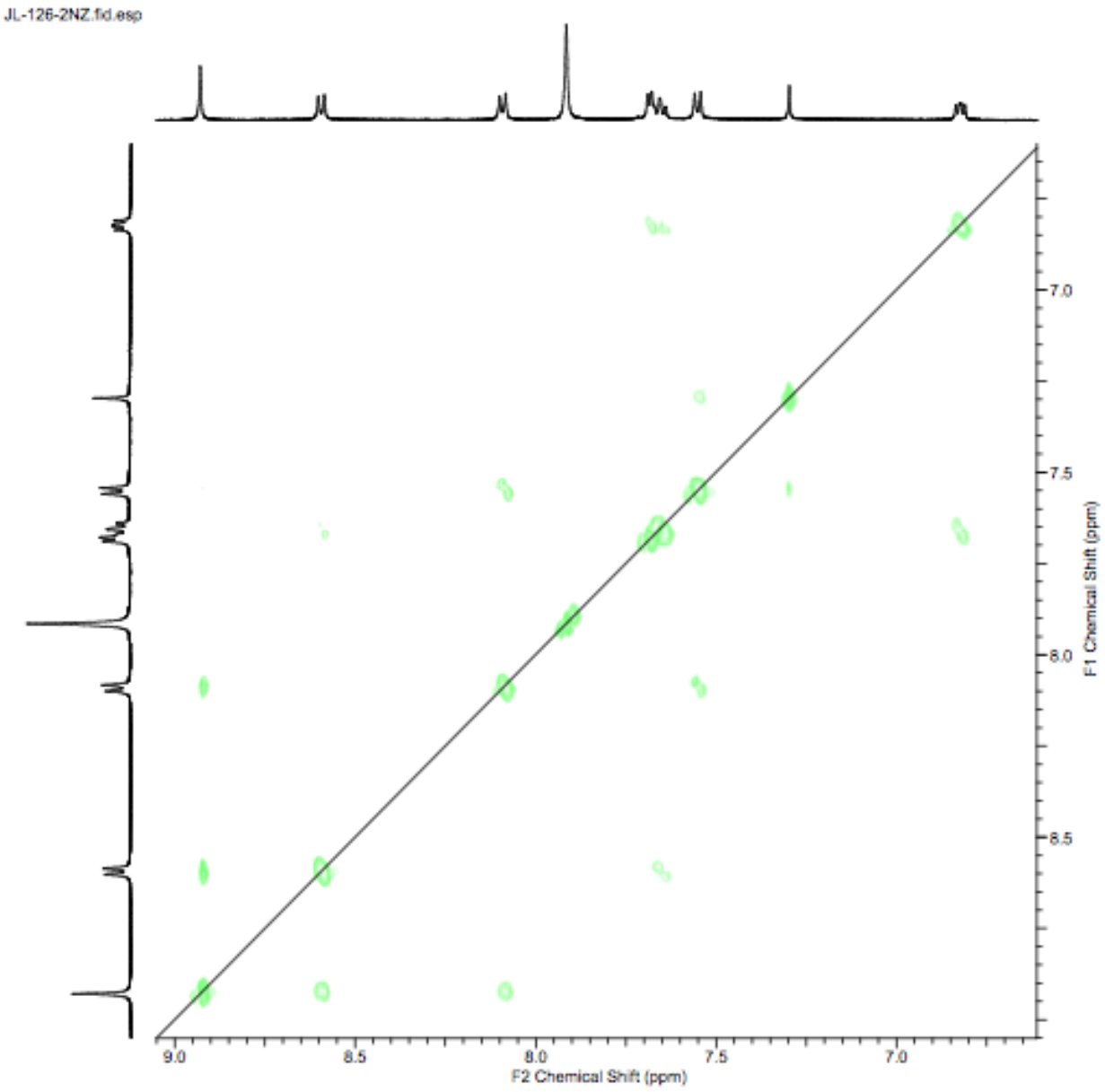

Figure S7. NOESY for **L4M12**, aromatic region CD_3CN/DMF-d_7.(5:1) at 0.6 mg/mL and 20 °C

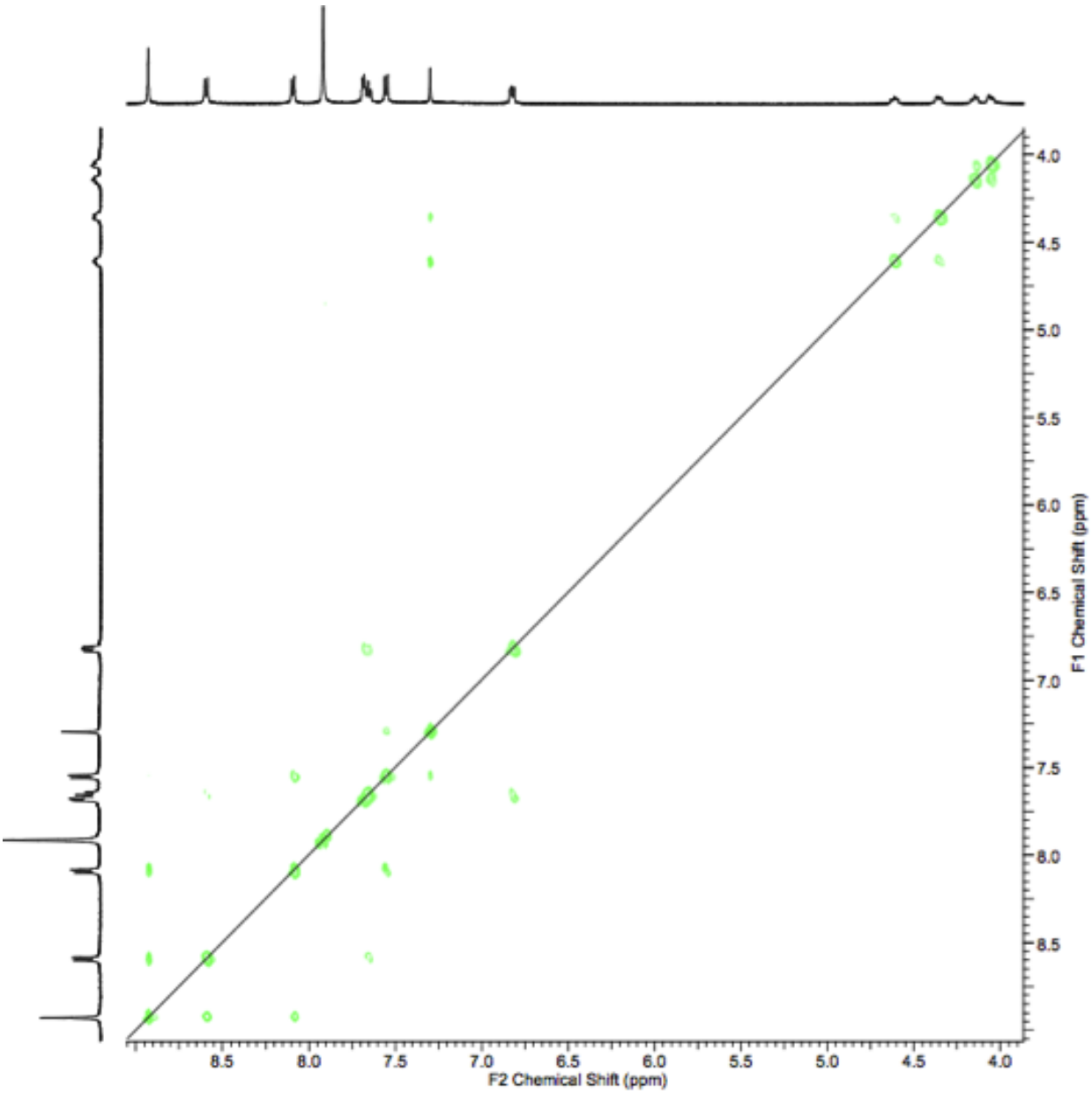

Figure S8. NOESY for **L4M12**, aromatic and marker region CD_3CN/DMF-d_7.(5:1) at 0.6 mg/mL and 20 °C

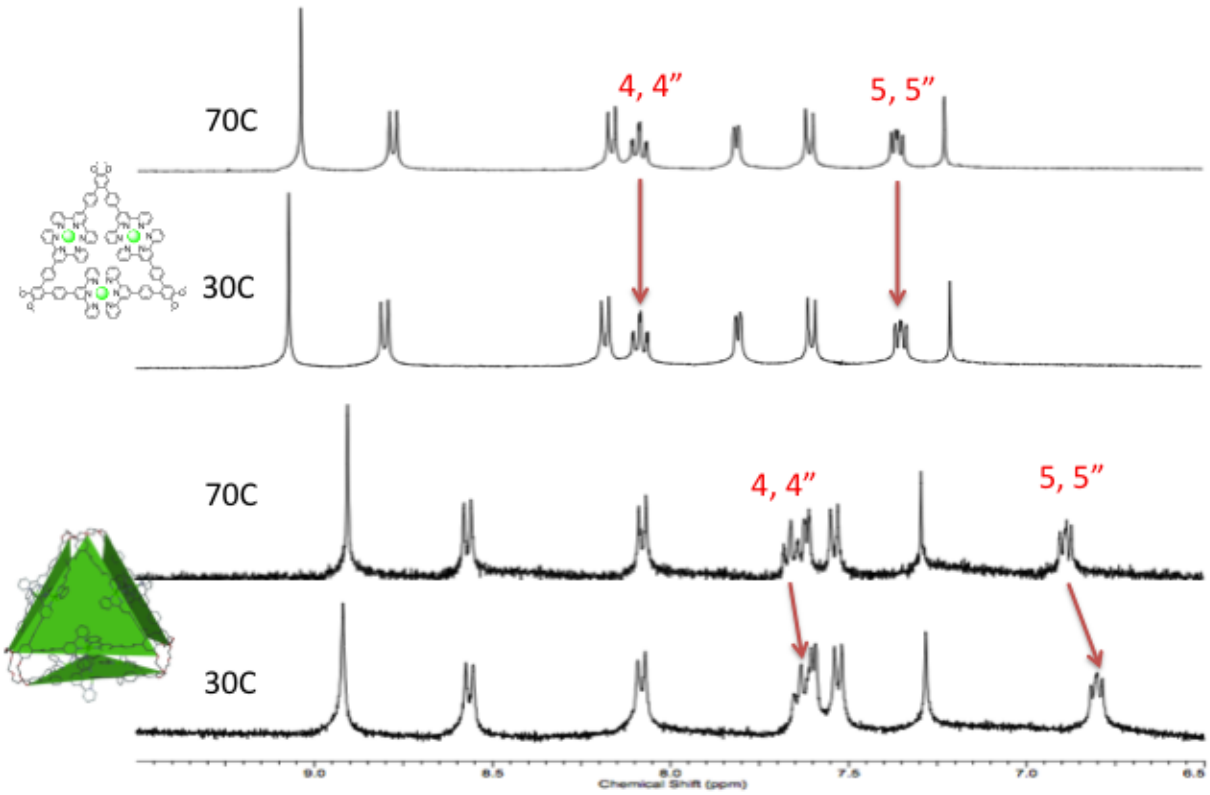

Figure S9. Variable temperature NMR of 'free triangle' **2** (3.0 mg/mL) and **L4M12** (0.6 mg/mL) CD_3CN/DMSO d_6 (10:1)

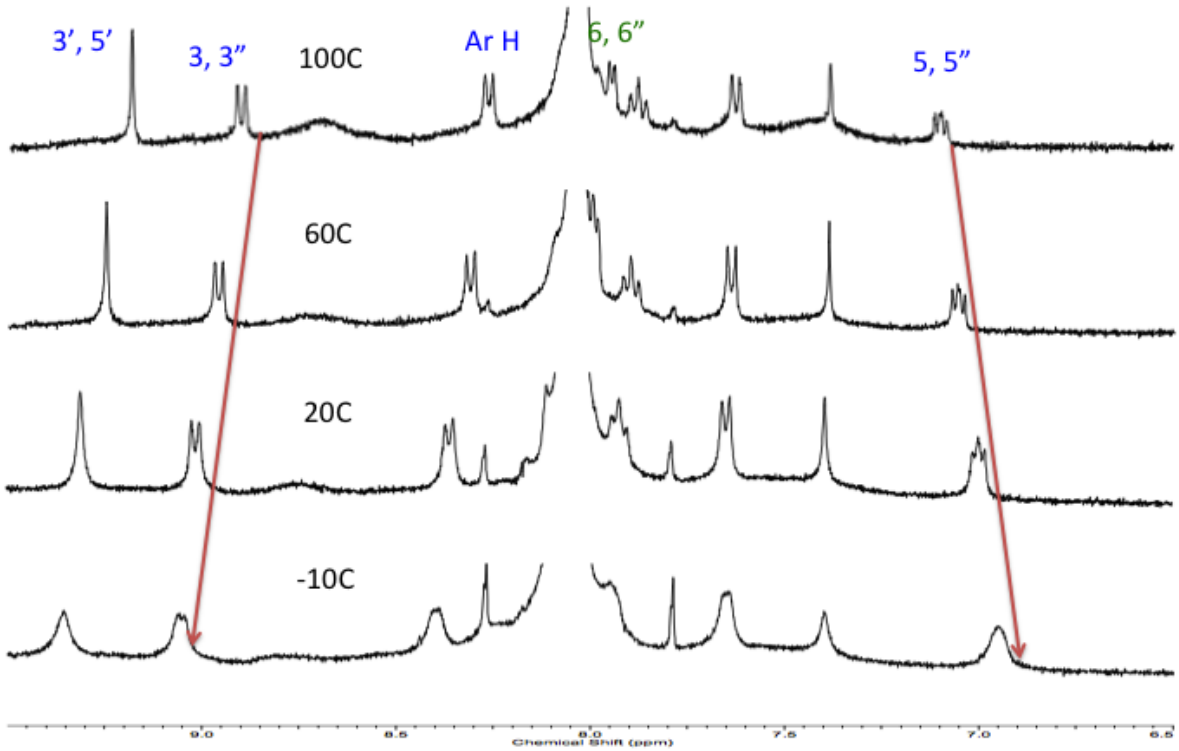

Figure S10. Variable temperature NMR of **L4M12** DMF-d_7

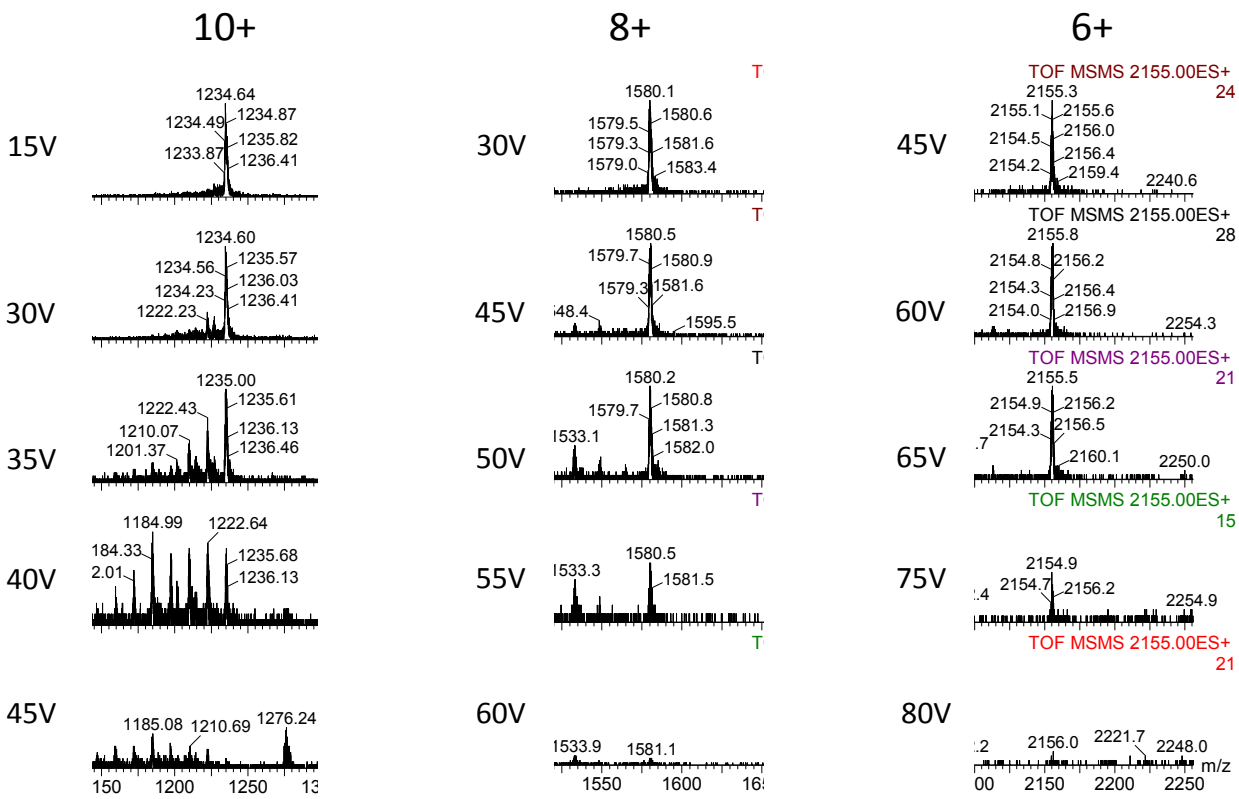

Figure S11. – gradient tandem mass spectrometry (gMS^2) results for 10+, 8+, and 6+ charge states of **L4M12**.

References.

1. S. J. Cantrill, M. C. T. Fyfe, A. M. Heiss, J. F. Stoddart, A. J. P. White and D. J. Williams, *Org. Lett.*, 1999, **2**, 61-64.
2. A. Schultz, Y. Cao, M. Huang, S. Z. D. Cheng, X. Li, C. N. Moorefield, C. Wesdemiotis and G. R. Newkome, *Dalton Trans.*, 2012, **41**, 11573-11575.
3. B. T. Ruotolo, J. Benesch, A. Sandercock, S.-J. Hyung and C. V. Robinson, *Nat. Protoc.* 2008, **3**, 1139-1152.